Received: 23 December 2020 | Revised: 11 March 2021 | Accepted: 4 April 2021

DOI: 10.1002/eco.2296

RESEARCH ARTICLE

WILEY

The hydrology of treed wetlands in thawing discontinuous permafrost regions

Brenden S. Disher[1] | **Ryan F. Connon**[2] | **Kristine M. Haynes**[3] | **Christopher Hopkinson**[4] | **William L. Quinton**[3]

[1]National Hydrological Services, Environment and Climate Change Canada, Saskatoon, Saskatchewan, Canada

[2]Environment and Natural Resources, Government of the Northwest Territories, Yellowknife, Northwest Territories, Canada

[3]Cold Regions Research Centre, Wilfrid Laurier University, Waterloo, Ontario, Canada

[4]Department of Geography and Environment, University of Lethbridge, Lethbridge, Alberta, Canada

Correspondence
Kristine M. Haynes, Cold Regions Research Centre, Wilfrid Laurier University, 75 University Ave. West, Waterloo, ON N2L 3C5, Canada.
Email: khaynes@wlu.ca

Funding information
Northern Scientific Training Program; Natural Sciences and Engineering Research Council of Canada; ArcticNet

Abstract

In peatland-dominated regions of discontinuous permafrost, widespread permafrost thaw has led to an expansion of treed wetlands on the landscape. Treed wetlands have greater topographic variation than the collapse scar wetlands from which they evolved, but their hydrological role in the landscape has not been identified. This study examines the development of treed wetlands, and characterises their physical, thermal and hydrological properties in relation to their adjacent peat plateaus and collapse scar wetlands. Electrical resistivity tomography was used to determine the geophysical characteristics of treed wetlands. Snow cover, soil moisture and temperature, as well as water level and storm response were monitored and compared in treed wetlands, plateaus and collapse scars. Treed wetlands were permafrost free, although unlike collapse scars they may contain multi-year ice bulbs. For treed wetlands, the late-winter snow water equivalent, average soil temperature and moisture, unsaturated layer thickness and duration of frozen ground were all intermediate between those of peat plateaus and collapse scars. Treed wetlands interact hydrologically with adjacent peat plateaus and collapse scars in one of two types of local flow sequences depending upon topographic position, which governs the potential role of treed wetlands as a thermal buffer if treed wetlands are situated between a collapse scar wetland and permafrost-cored peat plateau. As permafrost thaw reduces the cover of both peat plateaus and the collapse scar wetlands that develop from them, the development and expansion of treed wetlands appear to be transitioning plateau-wetland complexes into the permafrost-free black spruce forest.

KEYWORDS
hydrology, permafrost thaw, land cover change, treed wetlands

1 | INTRODUCTION

The Subarctic region is among the most rapidly warming on Earth (Payette et al., 2004; Tarnocai, 2009). Subarctic land covers are particularly vulnerable to climate warming-induced changes (Camill, 2005) since many of them are underlain by or adjacent to permafrost, which is at or near the melting point temperature of the ground ice and therefore susceptible to thaw and disappearance. The nature and rate of permafrost thaw-induced land cover transformations (Carpino et al., 2018) and the associated ecohydrological responses and feedbacks (Waddington et al., 2015) are poorly understood. In northwestern Canada, climate warming is rapidly degrading permafrost and changing the flux and storage of water and energy (Quinton et al., 2011; Shur & Jorgenson, 2007). In the discontinuous and sporadic permafrost zones, the occurrence of permafrost is often restricted to below relatively dry organic terrains since their low

thermal conductivity can preserve permafrost even where the mean annual air temperature (MAAT) approaches or exceeds 0°C (Shur & Jorgenson, 2007). Peat plateaus are ubiquitous throughout lowland regions of discontinuous permafrost. Their ground surfaces rise ~0.5 to 2 m above the surrounding permafrost-free, typically treeless wetlands, including channel fens and collapse scar wetlands (Beilman, 2001). This higher elevation allows plateaus to maintain an unsaturated layer needed to support both permafrost and a mature black spruce (*Picea mariana*) forest (Vitt et al., 1994).

Zoltai (1993) described a dynamic landscape of cyclic permafrost degradation (thaw) and aggradation (development) whereby peat plateaus develop from *Sphagnum spp*. hummocks that form above perennial ice bulbs (i.e., frozen ground that does not completely thaw during summer) within permafrost-free, treeless wetlands, while collapse scars form within plateaus and become permafrost-free wetlands. For a stable climate, the relative proportions of permafrost and permafrost-free terrains are assumed to remain relatively constant; however, the climate warming of recent decades appears to have disrupted this balance such that the rate of permafrost degradation exceeds that of permafrost development (Halsey et al., 1995). Permafrost thaw results in subsidence of plateau ground surfaces, inundation, loss of their canopy covers (Beilman et al., 2001; Quinton et al., 2011; Zoltai, 1993) and ultimately their conversion from forest to wetland with implications to drainage processes and pathways (Walvoord et al., 2019; Chasmer & Hopkinson, 2017; Connon et al., 2014, 2015), ecology (Beilman, 2001) and biogeochemical processes (Gordon et al., 2016) including carbon cycling (Helbig et al., 2016; Vonk et al., 2019).

Zoltai's (1993) conceptualisation of permafrost aggradation and degradation inspired subsequent investigations of landscape and ecosystem responses to permafrost change. For example, Camill (1999) reported that following the permafrost thaw-induced transformation of a peat plateau to a wetland, the new wetland surface is initially characterised by aquatic vegetation (e.g., *S. riparium*), which over time is replaced by a *S. angustifolium* lawn, followed by the development of more heterogeneous communities that include hummock-forming species (e.g., *S. fuscum*). The vertical development of hummocks provides an elevated surface above the local water table that is sufficiently dry to support black spruce seedlings (Lieffers & Rothwell, 1987). During winter, their higher topographic position limits the development of an insulating snow layer, and as a result, they are more exposed to the atmosphere than the inter-hummock terrain. Hummocks can therefore promote ice bulb formation during winter and can preserve them during summer (FitzGibbon, 1981; Nungesser, 2003). These effects are magnified as ice bulbs grow, since their growth may cause further vertical displacement of the ground surface and promote further growth of the black spruce seedlings, which both intercept snowfall and reduce insolation. Continued growth and coalescence of hummocks and their underlying ice bodies is thought to lead to the emergence of a peat plateau (Zoltai, 1993).

Much of the literature on permafrost thaw-induced changes of the type discussed above is focussed on the end-members of permafrost thaw (i.e., collapse scars and peat plateaus). Treed wetlands are often assumed to be a transitional stage between these two end-members and as such have received comparatively little attention. However, the disruption of the permafrost aggradation–degradation cycle by increased rates of permafrost thaw over recent decades, casts uncertainty on the trajectory of treed wetlands, including on how they have evolved and what they might be transitioning to. The relatively small height and circumference of the black spruce of treed wetlands compared to those of the plateaus (Haynes et al., 2020) suggests that these features evolved from treeless wetlands rather than directly from peat plateaus (Carpino et al., 2018). Moreover, the common observation of mature black spruce trees rooted in large hummocks suggests a synchronous growth of trees and the hummocks supporting them. Since the trees occur preferentially on hummocks, their distribution within treed wetlands is typically clustered, suggesting that such wetlands evolved as a result of local drying of sufficient magnitude to enable tree growth in certain areas. The trajectory of what treed wetlands are transitioning into is less clear. However, the common occurrence of permafrost-free terrain supporting black spruce forest in regions where the northward migration of permafrost thaw is well documented (e.g., Kwong & Gan, 1994) suggests that collapse scar wetlands are more likely to transition to treed wetlands than to peat plateaus (Carpino et al., 2018).

In recent years, there has been growing concern over the impacts of widespread permafrost thaw-induced land cover change on northern water resources (Government of the Northwest Territories [GNWT], 2018). The direction of hydrological change is not uniform across the discontinuous permafrost zone in the Northwest Territories. Some regions are experiencing increased landscape inundation, where interactions between subpermafrost groundwater and surface water are increasing particularly in spring and summer, causing community concerns on accessing the land and maintaining a traditional way of life. Other regions are experiencing surface water drainage with the loss of permafrost barriers, which act as impoundments and affects the geophysical and vegetation characteristics (GNWT, 2018). Since field observations suggest that treed wetlands develop following permafrost thaw, it is reasonable to expect that their coverage will increase in drainage basins where such thaw is widespread and resulting in the partial drainage of wetlands (Haynes et al., 2020). Understanding the hydrological functioning of treed wetlands and their hydrological interactions with adjacent land covers will provide new knowledge on how permafrost thaw affects the flux and storage of water within basins and how, more generally, this might affect northern water resources.

Although there is a dearth of literature on the hydrology of treed wetlands in permafrost terrain, studies on the hydrological functioning of the major land cover types that share such terrains with treed wetlands provide valuable insights. For example, the relatively high topographic position of peat plateaus prevents them from receiving hydrological input other than precipitation and enables them to function primarily as runoff generators (Quinton et al., 2003). Treed wetlands are often wrongly identified as peat plateaus owing to their tree cover and have therefore been assumed to overlie permafrost and to function hydrologically as peat plateaus. These wetlands

typically occupy an elevation below that of peat plateaus but above that of collapse scar wetlands. Collapse scar wetlands are thermokarst features in the form of permafrost-free depressions within peat plateaus (Robinson & Moore, 2000). Unlike plateaus, collapse scar wetlands receive lateral runoff (from adjacent plateaus) in addition to precipitation. Because their ground surface is below the elevation of the impermeable permafrost table of the surrounding peat plateau, these wetlands are impounded and unable to generate runoff, and as such, their hydrological function is primarily one of water storage. Channel fens are broad, linear wetlands oriented parallel to the mean topographic slope, with widths of tens to hundreds of metres (Vitt et al., 1994). Individual channel fens are separated from one another by peat plateau-wetland complexes, and their hydrological function is primarily to convey to the basin outlet the water they receive from direct precipitation and drainage from their adjacent plateau-wetland complexes (Quinton et al., 2003).

Further insight into the hydrological role of treed wetlands is gained from recent studies on how permafrost thaw is changing water flow and storage processes on the landscape. For example, permafrost thaw is driven by simultaneous vertical (from the ground surface) and horizontal (from adjacent permafrost-free terrains) energy fluxes, and as a result, the permafrost table deepens while plateau edges recede (McClymont et al., 2013). Once the permafrost table depth exceeds that of the annual re-freeze, a supra-permafrost talik develops, which enables continued permafrost thaw throughout the winter period, and provides a year-round subsurface drainage pathway (Connon et al., 2018; Parazoo et al., 2018). Receding plateau edges allow wetlands to expand and coalesce, a process that can transform wetlands from being hydrologically isolated from the basin drainage network to being connected to it. Connon et al. (2014) referred to this transition as wetland 'capture' and described one such process in which partial thaw of permafrost may generate ephemeral flowpaths between wetlands allowing water to cascade from one wetland to the next (Connon et al., 2015). The partial drainage of such wetlands (Haynes et al., 2018) is critical to the re-establishment of trees (Carpino et al., 2018; Chasmer & Hopkinson, 2017).

This study seeks to improve the understanding of the formation of treed wetlands, their hydrological functions and interactions with other land covers, and how they relate to the permafrost thaw-induced process of land cover change. This will be accomplished through the following specific objectives: (1) identify the presence (or absence) of ground ice or permafrost below treed wetlands; (2) characterise the snow cover, snowmelt, water table, soil moisture and temperature regimes of treed wetlands relative to peat plateaus and collapse scar wetlands; and (3) present a conceptual model that places treed wetlands in the context of permafrost thaw-induced land cover change and describes their hydrological function.

2 | STUDY SITE

Field studies were conducted at the Scotty Creek Research Station, approximately 50 km south of Fort Simpson, Northwest Territories, Canada (Figure 1a). Scotty Creek drains a 152-km^2 basin with a high concentration of peatlands and is underlain by discontinuous permafrost. The headwaters of the basin, where this study was conducted, are dominated by large peat plateau-wetland complexes separated by channel fens (Figure 1b,c), while the northern or downstream end is dominated by mineral soil uplands intermixed with low elevation peatlands. The MAAT for the period 1981–2010 at Fort Simpson is −2.8°C, with a mean January temperature of −24.2°C and a mean July temperature of 17.4°C. Mean annual precipitation (1981–2010) is 390 mm, with 149 mm (38%) falling in the form of snow. Annual total precipitation has remained relatively stable over the past 50 years (Meteorological Service of Canada [MSC], 2017). Permafrost in the basin is relatively warm (i.e., at or near the temperature of the freezing point depression) with an average thickness between 5 and 10 m (McClymont et al., 2013). The permafrost terrain is juxtaposed with permafrost-free wetlands in the form of channel fens and collapse scar wetlands. Peat plateaus (43.0%), collapse scar wetlands (26.7%), channel fens (21.0%) and lakes (9.3%) are the four main land cover types within the headwaters of the basin (Chasmer et al., 2010), each of which has distinctive vegetation communities (Robinson & Moore, 2000) and hydrological functions (Quinton et al., 2009). A more recent land cover classification revealed that treed wetlands (newly identified as a distinct land cover feature in this basin) represent approximately 12% of the landscape (Haynes et al., 2020). The areal coverage of treed wetlands is comparable to the current classified area of collapse scar wetlands (12%). Given their low-lying position and black spruce forest cover, treed wetlands were likely misclassified as either peat plateaus or collapse scar wetlands in previous land cover classifications in the Scotty Creek basin (Haynes et al., 2020). A complete description of the common land cover types characteristic of the plateau-wetland complexes and their hydrological functions can be found in Quinton et al. (2019), a description of site instrumentation can be found in Haynes et al. (2019) and a description of vegetation communities can be found in Garon-Labrecque et al. (2015).

3 | METHODS

3.1 | Site selection

Four undisturbed study sites were selected, each containing a treed wetland, collapse scar wetland and peat plateau (Figure 1c). Given the need to travel to all sites each day, this was the maximum number that could be managed. At Sites 1 and 2, the treed wetlands border a peat plateau and a collapse scar wetland on opposite sides, while at Sites 3 and 4, the treed wetlands are situated entirely within a collapse scar wetland and therefore do not border a peat plateau (i.e., a permafrost body). At each site, the plateau included areas exhibiting signs of permafrost thaw as evidenced by the presence of a talik and leaning trees (hereafter 'thawing plateau') and areas without indications of thermokarst (hereafter 'stable plateau').

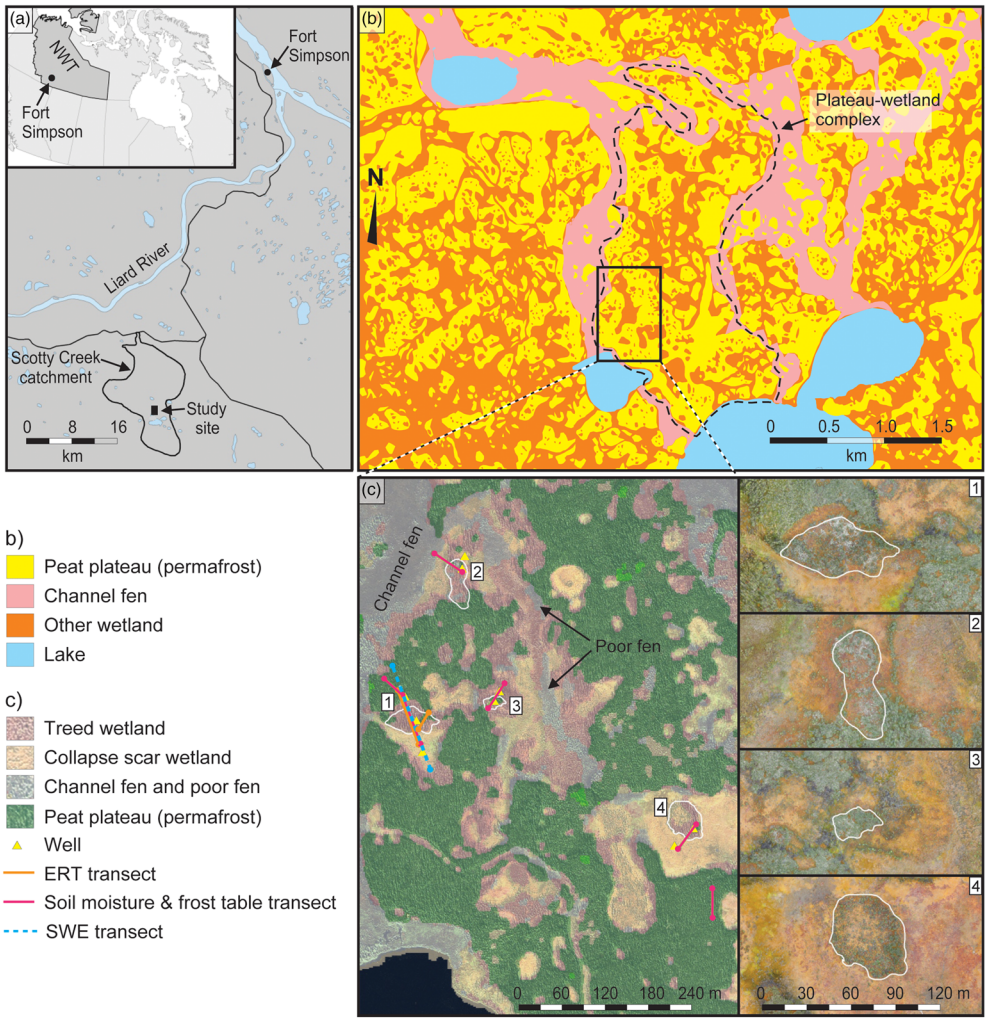

FIGURE 1 (a) Location of the study region in the Northwest Territories (NWT), Canada. (b) the headwater region of the Scotty Creek catchment indicating the plateau-wetland complex on which this study was conducted (modified from Quinton et al., 2019). (c) Aerial imagery (Worldview-2) indicating the measurement locations and the spatial distribution of the major land cover types. The high-resolution (UAV) images identify (within the white solid lines) the four treed wetlands examined in this study. Channel fens function as the main drainage network through the Scotty Creek basin. Classified channel fens developing within collapse scar wetlands are in the form of poor fens, with prolonged standing water and the establishment of sedge vegetation

3.2 | Geophysical investigation

Electrical resistivity tomography (ERT) measurements were conducted at Site 1 along two transects (Figure 1c). The first transect was 83 m long, traversed all three land cover types and was used to compare their substrates. The second transect was 28 m long and was used for a more detailed examination of the substrate below the treed wetland. ERT measurements are highly effective in permafrost environments due to the contrast in electrical resistivity between frozen and unfrozen materials (Kneisel et al., 2008). The ERT surveys involved the collection of resistivity values from a series of electrodes installed at 1-m intervals and connected to an AGI SuperSting 8-channel ERT control system. EarthImager 2-D Inversion Software was used to produce a cross section of the substrate from the resistivity measurements. Differential Global Positioning System (dGPS; Leica Viva Series, GS10) measurements were also made at each electrode. All measurements were conducted near the end of the thaw season (18 August 2018) when the active layer was fully thawed, so that frozen ground could be considered permafrost.

3.3 | Snowpack properties

At Site 1, a 175-m snow survey transect (Figure 1c) that traversed all three land cover types was used to measure snow depth and density every 2 or 3 days prior to the onset of snowmelt and every day thereafter. Snow depth was measured every 5 m, and snow density measurements were made every 10 m. Snow depth was measured by inserting a metal ruler to the base of the snowpack, and snow density was derived by weighing snow samples of known volume using an Eastern Snow Conference (ESC) 30 snow tube (30-cm^2 cross-sectional area; GeoScientific, Vancouver, BC, Canada). The depth and density measurements were used to compute average values of snow water equivalent (SWE) for each land cover type. Safe access to the study site was not possible late in the snowmelt period, and as a result, linear interpolation was used to estimate SWE following 26 April.

A remotely piloted aircraft (DJI Phantom 3 Professional) equipped with a digital camera (20-mm lens) was flown over the study sites daily throughout the snowmelt period starting on 23 April. The images were mosaicked using Pix4D (Pix4D Inc., Switzerland) at an image res-

olution of 0.035 m. An iso-cluster unsupervised image classification was used to distinguish between snow-covered and snow-free areas. Confusion matrices were computed for each day to test the accuracy of the unsupervised image classification using ArcGIS (Esri, Redlands, California). The snow-covered area (SCA) classification for each day was then overlain with a supervised image classification (Haynes et al., 2020) and used to estimate the percentage SCA for each land cover type for each day of the snowmelt period.

3.4 | Seasonal ground freeze and thaw

Immediately following the removal of the snow cover, the depth of refreeze that occurred during winter was measured by inserting a graduated steel frost probe vertically into the ground and through the entire thickness of the seasonally frozen layer following the method described by Connon et al. (2018). Briefly, the probe was first inserted to the depth of refusal. The probe was subsequently driven with force to incrementally breach the frozen active layer. The bottom of this layer is easily detected if it overlies a thawed (i.e., talik) layer, indicating permafrost thaw (i.e., thawing plateau). In cases where no talik was present, the depth of winter refreeze was assumed equal to the depth of summer thaw, indicating no permafrost thaw (i.e., stable plateau). These measurements were taken at 10-m intervals along the ERT transect (Site 1), as well as at 5-m intervals along the 50-m-long soil moisture transects at Sites 2–4 (Figure 1c). The depth of thaw was then measured daily at the same points of the aforementioned transects by inserting the frost probe vertically through the ground surface to the frost table (i.e., top of the seasonally frozen layer). In each land cover of Site 1, ground temperature was measured using Decagon 5TM temperature sensors at 5, 10, 15, 20 and 25 cm below the ground surface and connected to an EM50 data logger (METER Environment, Pullman, WA, USA), which recorded measurements every 30 min. The accuracy of the temperature sensors was ±1°C.

3.5 | Soil moisture

Volumetric water content (VWC) was measured every second day at 5-m intervals along each soil moisture transect (Figure 1c) using a handheld Hydrosense II (Campbell Scientific, Edmonton, AB, CAN) with a 20-cm probe. The probe was inserted vertically into the ground to yield estimates of the depth-integrated VWC over the 0- to 20-cm depth layer. At each interval, four measurements were taken, one in each cardinal direction 20 cm from the transect point. This provided an average value for each measurement interval. These measurements were also made at 20 additional points along the ERT transect (Figure 1c) at points identified as thawing plateau (see section above). In addition to these transect measurements, VWC was also measured in profile at the same locations and time intervals as the temperature profiles described above (i.e., the 5TM sensors measure both temperature and volumetric moisture content). The calibrations applied to HydroSense II and the 5TM probes were based on laboratory measurements performed on intact wetland and plateau peat samples (~10 × 10 × 30 cm) collected at Scotty Creek. Soil moisture values were monitored as the peat samples were incrementally wet and subsequently dried to develop gravimetric-based calibration algorithms specific to the peat in this basin, similar to the approach of Bourgeau-Chavez et al. (2010).

3.6 | Water level trends and event recession

Nine, 1.5-m-long, slotted polyvinylchloride (PVC) wells were instrumented with HOBO U20 pressure transducers (Hoskin Scientific, Edmonton, AB, CAN) and distributed at the four study sites such that a well was installed in each of the four treed wetlands and collapse scar wetlands, with the remaining well on a single plateau at Site 1 (Figure 1c). The wells were installed in the peat and anchored to the underlying mineral substrate with iron pipe to ensure that the measurements were not impacted by wetland surface oscillations. Absolute pressure was measured and recorded at 30-min intervals. Atmospheric pressure was measured using HOBO U20 pressure transducers installed in a non-slotted (i.e., dry) PVC well which was vented to the atmosphere and maintained a temperature similar to that of the pressure transducers in the slotted wells. Atmospheric pressure was subtracted from the absolute pressure to calculate water depth above each sensor. At each well, dGPS (±2 cm) measurements were used in order to express water table elevations in values of metres above mean sea level (masl). Water table recession rates were computed using the approach of Tallaksen (1995) and applied to peatland water table recessions by Menberu et al. (2016) and Bourgault et al. (2017):

$$Q_t = Q_o e^{-at}, \quad (1)$$

where Q_t is the water table elevation (masl) at time t after the start of the recession, Q_o is the water table elevation (masl) at the start of the recession, e is the natural logarithm, a is the recession coefficient (day^{-1}) and t is time (day). Four precipitation events in 2018 were selected for which mean recession coefficients were calculated for each of the three monitored land cover types. These precipitation events were chosen to compare event recession among the three land cover types as they were of similar magnitude (~13–22 mm) and were the largest events of the 2018 study period that triggered a notable water level response in each site. Recession coefficients for each event were evaluated using a minimum of a 5-day recession period. A master recession curve (MRC) representing a compilation of multiple recessions into a single curve (Posavec et al., 2006) was defined for each land cover type to provide an average, land cover-specific characterisation of hydrological response. Rainfall was measured using a tipping bucket rain gauge at a meteorological station located in a wetland between Sites 2 and 3. This rain gauge was connected to a CR1000 data logger (Campbell Scientific, Edmonton, AB, Canada) and records the total number of tips (0.25 mm per tip) over 30-min intervals.

3.7 | Statistical analyses

All statistical analyses were completed using R statistical software (R Core Development Team, Version 3.5.2, 2018). Level of significance (α) for statistical comparisons was set to $\alpha = 0.05$. All data were tested for normality (Shapiro–Wilk W test) and log-transformed when parametric assumptions were not met. Mean SWE and recession slope were compared among the land cover types using one-way analysis of variance tests with post hoc Tukey tests. In the case of the thickness of the seasonally frozen layer, a Welch one-sided test was used because the variance of these values was not equal among the sites.

4 | RESULTS

4.1 | Geophysical characteristics

For Transect 1, the relatively low resistivities (<500 Ωm) in the upper 50 cm of peat on the plateau resulted from the absence of ice in the active layer, which was entirely thawed at the time of the survey (Figure 2a). The high resistivities (>5000 Ωm) directly below the active layer reflect the high ice content of the underlying permafrost, the presence of which was confirmed by frost probe measurements. By contrast, low resistivity below the collapse scar and treed wetland ground surfaces resulted from the absence of permafrost. The discontinuity below 2.5 m indicated a transition from peat to mineral sediment, which was confirmed by drilling boreholes and was consistent with previous ERT measurements at the study site (McClymont et al., 2013).

With the exception of the values between electrodes 21 and 28, high resistivity values (>5000 Ωm) were largely absent from Transect 2. The high resistivity between electrodes 21 and 28 suggested the presence of ice bulbs below hummocks, which was confirmed independently by frost probe measurements (Figure 2b). Frost probe measurements also indicated that the ice bulbs below and adjacent to Transect 2 had an average depth of 59 ± 12 cm below the hummock ground surface (range of 44 to 84 cm below ground surface) and had an average thickness of 13 ± 6 cm ($n = 8$), ranging in thickness from 8 to 24 cm.

4.2 | Snowpack characteristics

Prior to the onset of snowmelt (23 April, 2018), the peat plateaus had the greatest snow depth (65 ± 5 cm; mean ± standard deviation [SD])

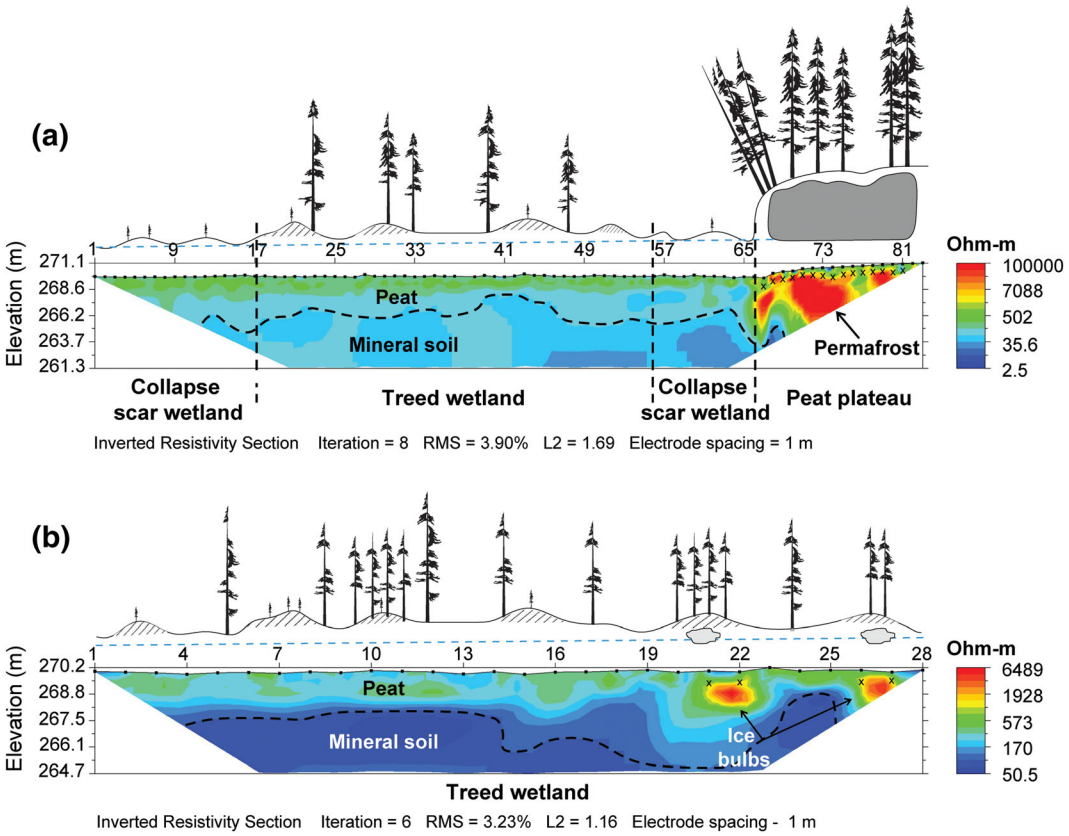

FIGURE 2 Electrical resistivity tomography (ERT) transects for Site 1. (a) Transect 1 (83 m) includes all three land cover types. (b) Transect 2 (28 m) measures only a treed wetland. Note the difference in scale between the two plots. Representation of vegetation on each transect is an illustration of approximate vegetation differences among land cover types. Measurements were completed in August 2018

and SWE (117 ± 18 mm; mean ± SD), while the collapse scar wetlands had the lowest snow depth (57 ± 5 cm) and SWE (97 ± 11 mm). These differences were weakly significant ($p = 0.06$). The treed wetlands had an average snow depth of 59 cm (±7 cm) and an average SWE of 105 mm (±10 mm) and were not significantly different from the other land cover types ($p = 0.3$ and 0.6 for comparisons with plateaus and collapse scar wetlands, respectively). By the final day of SWE measurements on 26 April, the peat plateaus had the greatest remaining SWE (54 ± 21 mm), followed by the treed wetlands (50 ± 14 mm), and finally the collapse scar wetlands (42 ± 18 mm). These values were not significantly different ($p = 0.6$ comparing plateau and treed wetland; $p = 0.8$ comparing plateau and collapse scar; $p = 0.9$ comparing treed wetland and collapse scar). During the first 5 days of the snowmelt period (22–26 April), the melt rate was highest in the collapse scars, lowest in the plateaus and intermediate in the treed wetlands. The collapse scars were also the first feature to become snow free, followed by treed wetlands and finally plateaus (Figure 3). By the date of the final SCA measurements (1 May 2018), snow covered 33% of the plateau ground surfaces, and only 17% and 3% of the treed wetland and collapse scar wetland ground surfaces, respectively. The overall accuracy of the SCA estimate on 25 April was 88% (Kappa = 0.76) and increased to 98% for the remaining days.

4.3 | Seasonal ground freeze and thaw

Peat plateaus with indications of permafrost thaw (e.g., subsided terrain, leaning trees and talik presence) had the greatest average depth of refreeze (60 ± 10 cm; mean ± SD). There was a highly significant difference in re-freeze depths between collapse scar wetlands (38 ± 7 cm) and both forested land cover types (both $p < 0.001$), but not ($p = 0.6$) between treed wetlands (56 ± 13 cm) and plateaus (60 ± 10 cm). Furthermore, during the winter period, ground temperatures (10 cm below the surface) of treed wetlands and peat plateaus were of similar magnitude (Figure 4a) and followed a similar trend, particularly during the later winter months (Figure 4b).

The over-winter ground thermal regimes of plateaus and collapse scars have been well described (e.g., Hayashi et al., 2007) so was not further investigated here. However, the temperatures below these land cover types provide a frame of reference to evaluate the thermal regime below treed wetlands. Figure 4 shows that unlike the other land cover types, the treed wetland has three distinct thermal stages during winter. Stage 1 includes the transition from the zero-curtain condition when temperatures are fixed at the freezing point depression (~ −0.2°C) to the subsequent stages of variable temperature (Figure 4b). Stage 2 represents the early winter when the temperature variations of the treed wetland mirror those of the collapse scar wetland. Stage 3 represents the late winter when the temperature variations of the treed wetland mirror those of the peat plateau.

Throughout the winter period, the collapse scar maintains the highest average temperatures (mean = −0.3°C, SD = 0.2°C), followed by the treed wetland (mean = −1.0°C, SD = 0.7°C) and the peat plateau (mean = −1.8°C, SD = 0.6°C). At the end of winter, the collapse scar wetlands thawed the quickest, losing their ground ice within 1–3 weeks of snowmelt, while ground ice within the treed wetlands persisted much longer throughout the summer, with six of the 20 measurement points retaining ice for the entire summer.

4.4 | Soil moisture

Early in the ground thaw season (18 May), the average VWC values integrated over the 0- to 20-cm-depth range were highest in the collapse scar wetlands (mean = 68%, SD = 2%), followed by plateaus where permafrost is thawing as evidenced by the presence of taliks (mean = 58%, SD = 4%), treed wetlands (mean = 38%, SD = 4%) and peat plateaus not exhibiting permafrost thaw (VWC mean = 30%,

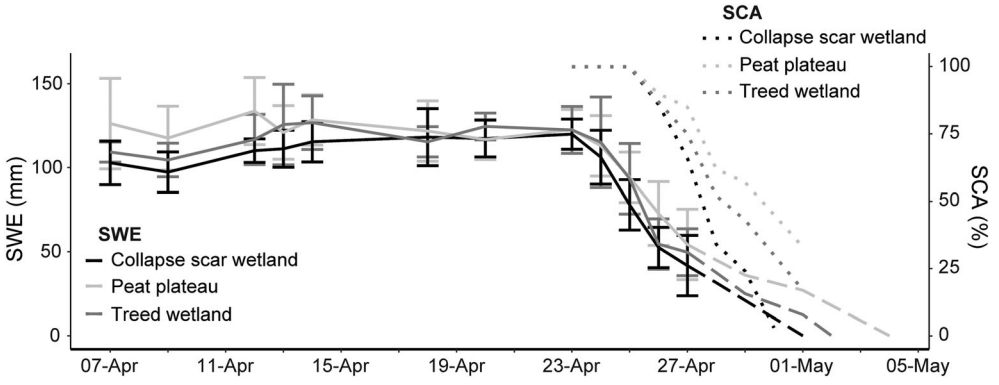

FIGURE 3 Snowpack snow water equivalent (SWE; solid lines) and snow-covered area (SCA; dotted lines) measurements at Site 1. Snowmelt commenced on 23 April. Pre-melt measurements were taken for approximately 15 days, while melt measurements were taken for 5 days. The error bars represent the standard deviation of the average SWE measurement for each land cover type. After the final measurement (26 April), linear interpolation was used to complete melt for each feature and is denoted with the dashed line. It should be noted that the snow-free day for each land cover type is approximated to ±1 day using areal imagery. Snow covered area (SCA %) is plotted near the end of the period to depict the areal loss of the snowpack

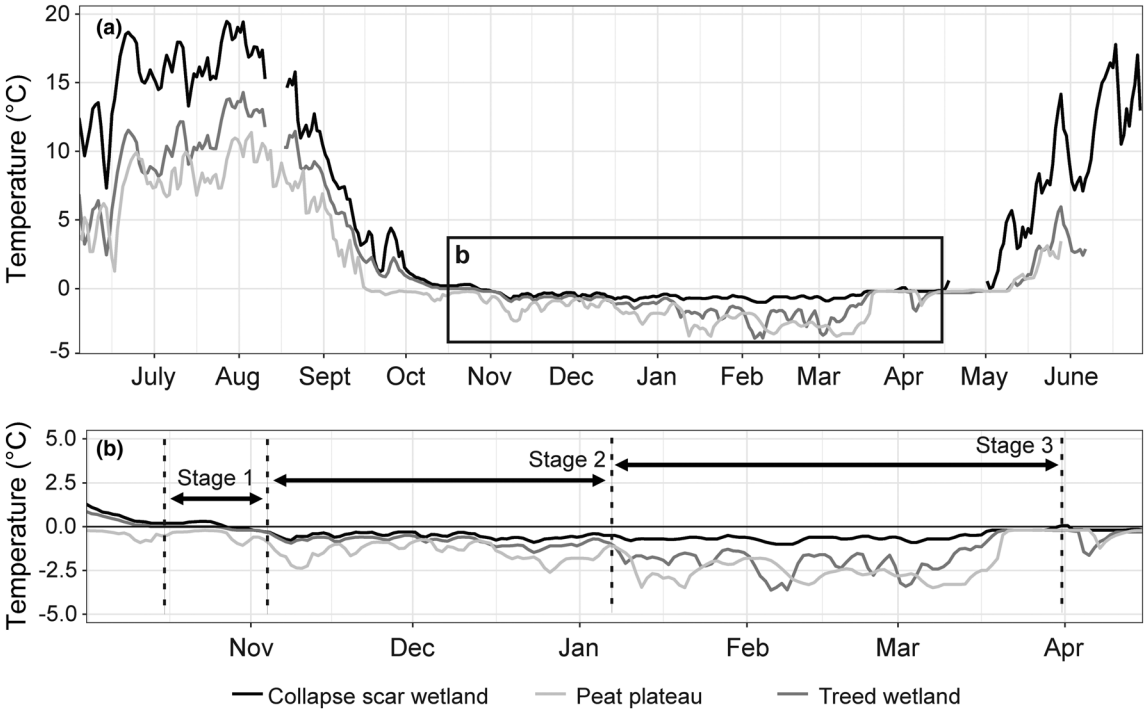

FIGURE 4 Daily average ground temperatures measured at 10-cm depth at the peat plateau, treed wetland and collapse scar wetland of Site 1 for (a) the period from 3 June 2018 to 27 June 2019 and (b) the period from 1 October 2018 to 15 April 2019 including the winter

SD = 4%). Differences in mean VWC were significant between land cover types ($p < 0.05$, with most < 0.001), except between treed wetlands and locations on plateaus overlying a talik ($p = 0.9$). The collapse scar wetlands maintained the highest VWC (>60%) throughout the measurement period, while the peat plateaus (without permafrost thaw) remained the driest. Treed wetlands maintained VWC values between peat plateaus and collapse scar wetlands, while thawing plateau locations had higher VWC than treed wetlands.

The soil moisture profiles of each land cover type at Site 1 demonstrate characteristic summer and winter VWC regimes, with relatively little variation within each type and season except in early summer when ground thaw, being a time-dependant process, resulted in variations of VWC within and between land cover types (Figures 5 and S1). During summer, the collapse scar wetland maintained the highest VWC among the sites and a constant, saturated value at all depths. The near-surface depths (5, 10 and 15 cm) show the response to an irregular early spring snowmelt event in mid-March that thawed the soil and was followed by soil re-freeze (Figure 5). The plateau site had the lowest VWC among the sites with unsaturated values at all depths, although values temporarily approached saturation at 25-cm depth in response to precipitation. At the treed wetland, summer VWC values in the upper 15 cm were intermediate between those of the plateau and collapse scar wetland, but values at 20- and 25-cm depths approached saturation and therefore closely matched the values at the collapse scar wetland (Figure 5). Ground freezing in the treed wetlands lagged behind that in collapse scars (Figure S1). This was expected given the drier near-surface peat of the former, which would have restricted heat loss in early winter. Regardless of the VWC prior to freeze-back in the fall, the winter VWC values of all sites converged to approximately 0.2, representing the residual liquid moisture in the otherwise frozen peat (Quinton et al., 2005). The VWC of the plateau was slightly lower than the other sites, reflecting the lower availability of moisture prior to freeze-back. At the end of winter, the wettest site (collapse scar wetland) thawed first, and the driest (plateau) thawed last (Figure S1).

4.5 | Water level trends and event recession

At Site 1, the water table of the peat plateau remained perched above those of the adjacent collapse scar and treed wetland throughout the study period. Manual measurements confirmed the same at the other three study sites. At all four sites, the water table of the treed wetlands remained above the collapse scar wetland (Figure 6). As such, the hydraulic gradient at all sites was directed from treed wetland to the collapse scar, and at sites where plateaus and treed wetlands were contiguous (Sites 1 and 2), the hydraulic gradient was directed from the plateaus to the treed wetlands. Figure 6 also shows that the water table remained closer to the ground surface at the collapse scar wetlands (mean depth = 9 cm) than at the treed wetlands (mean depth = 12 cm), indicating a greater unsaturated layer thickness at the treed wetlands although this difference was not statistically significant ($p = 0.3$). The rate of water table rise in response to precipitation was indistinguishable among the land cover types ($p = 0.2$). However, the recession coefficients of the plateau well were an order of

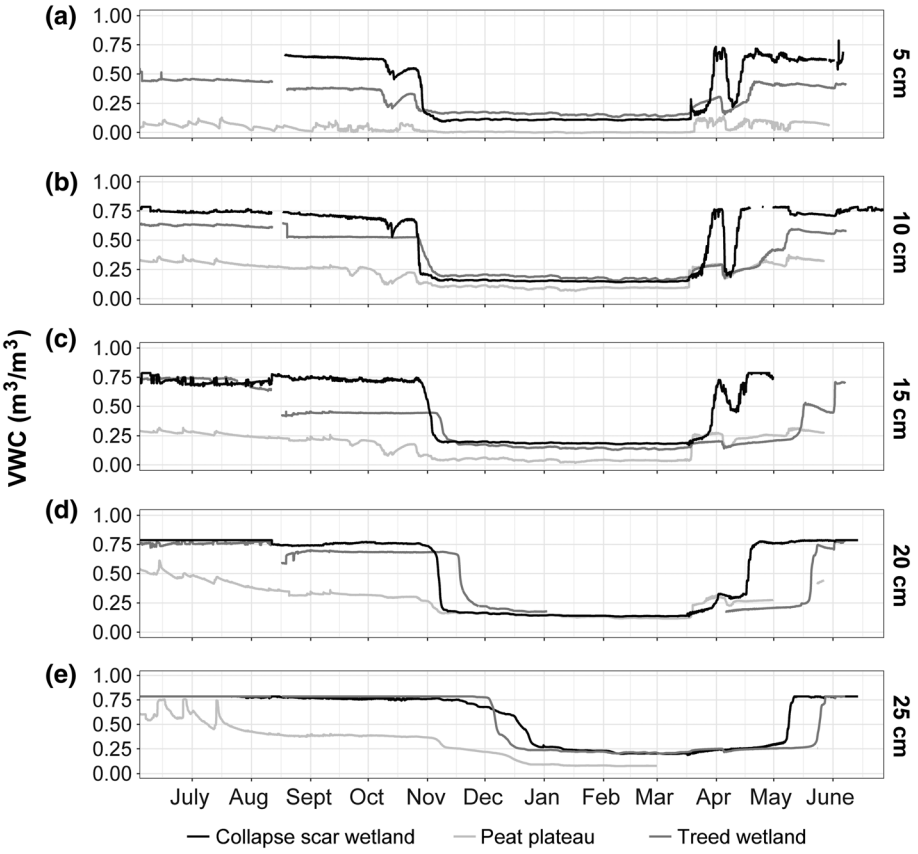

FIGURE 5 Continuous soil moisture VWC (m^3/m^3) recorded at five discrete depths (5, 10, 15, 20 and 25 cm) for each land cover type at Site 1. Data were collected for 1 year between June 2018 and June 2019. Data prior to mid-August were removed at 5 cm from the collapse scar wetland due to contact issues with the sensor, and the abrupt changes in VWC at all depths in mid-August occurred due to the sensors being disturbed and restored less than a week later

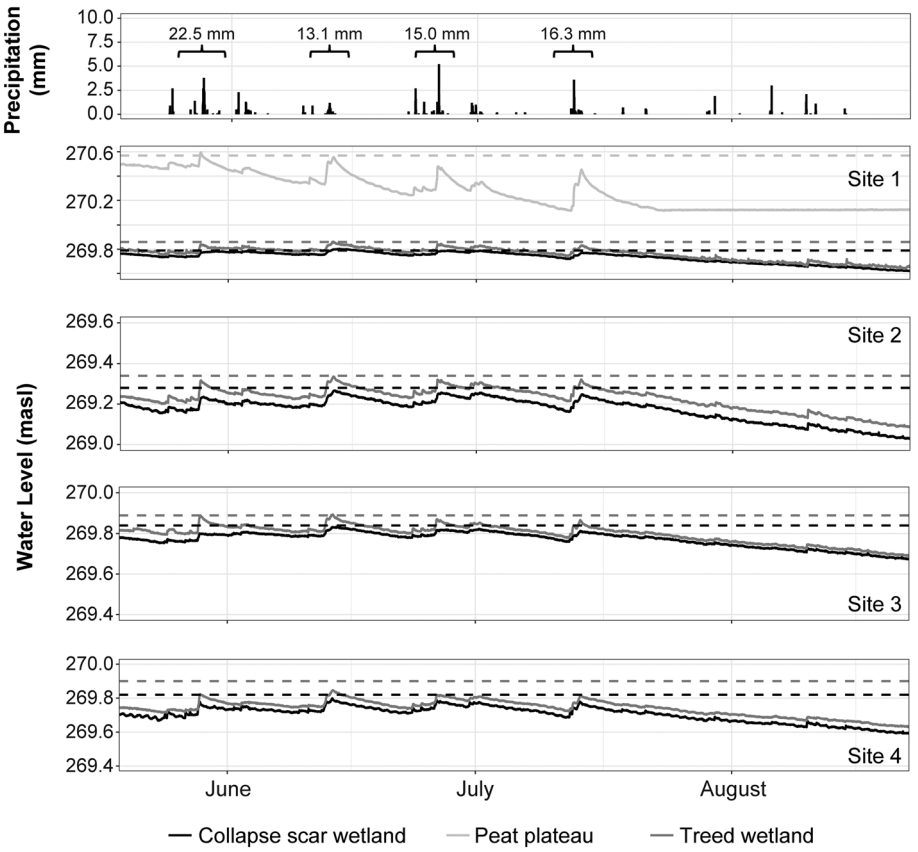

FIGURE 6 Water table elevation of the treed and collapse scar wetlands at the four study sites and the peat plateau at Site 1. The dashed lines indicate the elevation of the ground surface of the peat plateau (light grey), treed wetlands (dark grey) and collapse scar wetlands (black)

magnitude higher than those of the other land cover types for all four precipitation events examined (Table 1). Although the recession coefficients of the treed and collapse scar wetlands for the four events examined were of the same order of magnitude, those of the former were consistently and significantly ($p < 0.001$) higher. With the exception of Site 4, the mean recession curve trend lines were steeper and returned to the pre-event condition sooner as indicated by a shorter duration. Later in the summer season, the water table response to small precipitation inputs (as compared to the four examined events) is more muted for all land cover types in all sites (Figure 6). The inputs from small late-summer precipitation events contribute to storage deficits in these sites and therefore do not trigger a notable water level response.

5 | DISCUSSION

5.1 | Subsurface characteristics

The ERT measurements provided no indication of permafrost beneath treed wetlands. Previous ERT studies at Scotty Creek (McClymont et al., 2013) and in other regions of discontinuous permafrost (Lewkowicz et al., 2011) reported resistivity values for wetlands and plateaus similar to those reported in the present study. McClymont et al. (2013) also reported resistivities in excess of 5000 Ωm for the permafrost bodies beneath plateaus, as reported here for Transect 1. By contrast, Lewkowicz et al. (2011) reported much lower resistivity values (∼2000 Ωm), which they attributed to high liquid moisture contents characteristic of thawing permafrost. McClymont et al. (2013) reported resistivities of less than 100 Ωm for the mineral sediment below the ∼10-m permafrost bodies and below the wetlands, findings that are consistent with the present study. ERT surveys also indicated ice bulbs were present in treed wetlands but absent in collapse scars, suggesting that the thermal conditions provided by hummocks enabled the formation and preservation of ground ice. Not all hummocks in treed wetlands contained ice bulbs though, suggesting that there are local, site-specific conditions required for the development and persistence of ice bulbs. Ice bulbs may contribute to the stability of hummocks, and by extension, their ability to support trees, in a manner described by Zoltai (1993).

5.2 | Snowpack characteristics

Of the three land cover types, peat plateaus retained the highest SWE values by the end of winter (Figure 3). Their sparse, black spruce canopies although ineffective at reducing snow accumulation on the ground by canopy interception (Quinton et al., 2019) can reduce the horizontal wind speeds below the values measured over adjacent (treeless) wetlands (Haynes et al., 2019). The results of the present study suggest that this reduction is sufficient to limit wind erosion of the plateau snowpack. Treed wetlands contained greater end of winter SWE than collapse scar wetlands for the same reason, but the sparser and more spatially variable tree cover of the treed wetlands (Haynes et al., 2020) allowed greater loss of snow by wind erosion than on the peat plateaus. The three land cover types also demonstrated contrasting snowmelt rates. As open environments, the collapse scar wetlands would receive greater energy input from both insolation and aerodynamic (i.e., turbulent) fluxes (Marks et al., 1998) and therefore experienced a relatively early onset and completion of snowmelt resulting in a rapid decrease in SCA (Figure 3). On average, insolation on snow or ground surfaces of the plateaus is between 50% (stable plateau) and 80% (thawing plateau) of that incident upon collapse scar wetland surfaces owing to shading by the tree canopy (Connon et al., 2018). As a result, the rate of snowmelt and reduction in SCA was relatively low for the plateaus (Figure 3). Although insolation was not measured on treed wetlands, the intermediate level of black spruce cover as compared to forested peat plateaus and virtually tree-free collapse scar wetlands (Haynes et al., 2020) suggests that insolation would be intermediate between the values of the plateaus and collapse scar wetlands. For this reason, the intermediate rate of snowmelt and reduction in SCA of the treed wetlands was anticipated (Figure 3).

5.3 | Hydrological functioning of plateau wetland complexes

Plateau-wetland complexes contain numerous discrete peat plateaus, treed wetlands and collapse scar wetlands of varying size and shape. Within such complexes, the different land cover types self-organise into discrete hydrological groupings, which define a local sequence of flow between adjacent land covers (Connon et al., 2015; Gordon

TABLE 1 The 2018 precipitation (P) events that triggered a notable water level response and the corresponding mean recession coefficient of treed wetlands (TW), collapse scar wetlands (CSW) and the peat plateau (PP)

			Recession coefficient		
Event	P (mm)	Date	TW (day^{-1})	CSW (day^{-1})	PP (day^{-1})
1	22.5	28-May-18	3.4×10^{-5}	1.9×10^{-5}	1.30×10^{-4}
2	13.1	13-Jun-18	3.3×10^{-5}	2.8×10^{-5}	1.55×10^{-4}
3	15.0	26-Jun-18	3.0×10^{-5}	2.5×10^{-5}	1.98×10^{-4}
4	16.3	14-Jul-18	3.3×10^{-5}	2.7×10^{-5}	2.07×10^{-4}
		Mean	3.3×10^{-5}	2.5×10^{-5}	1.73×10^{-4}

Note: The mean values for each land cover type are also provided. The dates indicate the start of the precipitation event (see Figure 6).

et al., 2016). We suggest two general types of flow sequences that route water to collapse scars, the land cover of lowest elevation within plateau-wetland complexes. Type 1 flow sequences involve three contiguous land covers, a plateau at the highest elevation, a collapse scar wetland at the lowest and a treed wetland situated between the two. Type 2 flow sequences involve just two contiguous land covers and include both plateau to collapse scar, and treed wetland to collapse scar sequences (Figure 7).

By occupying the upslope end of the Type 1 flow sequences, plateaus receive no hydrological input other than from precipitation, are relatively well drained and exhibit a well-developed unsaturated layer. Plateaus shed water down-gradient to treed wetlands, which form a hydrological buffer between plateaus and the collapse scar wetland further down gradient. Unlike plateaus, the treed wetlands receive runoff from upslope (plateaus) and provide runoff to the collapse scar wetlands downslope. The greater topographic (and therefore hydraulic) gradient between the plateaus and treed wetlands than between the latter and collapse scars contributes to the higher VWC of treed wetlands than plateaus. Since collapse scar wetlands occupy the lowest elevation in both flow sequence types, and because they either have no runoff outlet, or have an ephemeral outlet that conveys water only during periods of high moisture supply, their VWC is typically the highest of any flow sequence. Type 2 sequences offer a more direct (i.e., not buffered by a treed wetland) transfer of water to collapse scars where they are directly adjacent to a plateau (Figure 7). Treed wetland to collapse scar sequences would transfer less water given the relatively low hydraulic gradient between the two cover types and the lack of a peat plateau to provide hydrological input from upslope.

Recent studies (e.g., Connon et al., 2015) demonstrated that permafrost thaw along the edges of some collapse scars has allowed them to partially drain into channel fens, either directly or through a hydrologically-connected series of collapse scars with thawing edges. Haynes et al. (2018) suggested that this permafrost thaw-induced partial drainage can catalyse the transition of collapse scars (or parts thereof) to treed wetlands. Channel fens and collapse scars that are directly adjacent to peat plateaus are a significant source of heat for permafrost thaw (Devoie et al., 2019). A treed wetland located between a plateau and a channel fen or between a plateau and collapse scar, can also function as a thermal buffer, as evidenced by its lower ground temperatures (Figure 4) and longer period of frozen ground (Figures 5 and S1) compared with collapse scar wetlands.

Notwithstanding permafrost thaw, several studies have reported a net vertical rise of the ground surface of collapse scars resulting from the growth of hummock-forming *Sphagnum* spp. (Camill et al., 2001; Jorgenson et al., 2010) and the colonisation of hummocks by other species, including black spruce, that require relatively dry conditions (Beilman, 2001). These studies suggest that collapse scars evolve into treed wetlands over several decades. The present study demonstrates the changes in peatland hydrological functioning that arise from this evolution of peatland form. For example, the transition to a treed wetland involves a drying of the near-surface peat, a condition required to support a tree root network. The observation that at the end of winter the wettest site (collapse scar wetland) thawed first and the driest (plateau) thawed last (Figure 4) demonstrates the profound effect of moisture content on ground temperatures and the ground thaw rate. Even though the treed wetland and collapse scar were both saturated at the 20- and 25-cm depths, the peat above

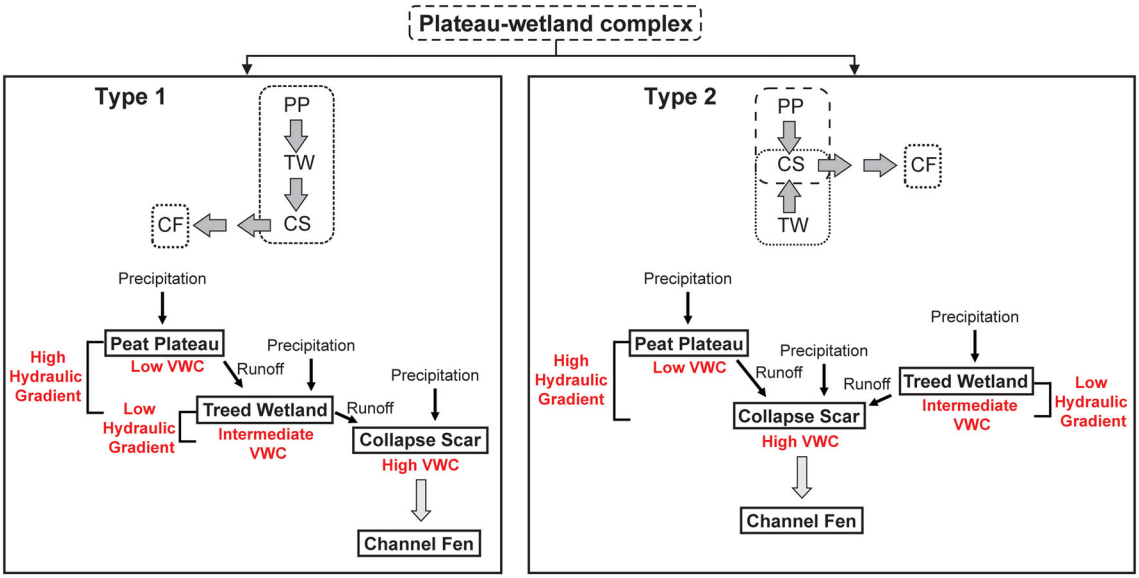

FIGURE 7 Conceptualisation of water redistribution of subsurface runoff from plateau-wetland complexes to channel fens and within such complexes via Type 1 and Type 2 land cover connections. The cross-sectional representations illustrate the relative topographic positions (and therefore hydraulic gradients) of peat plateaus, treed wetlands and collapse scar wetlands associated with both Type 1 and Type 2 land cover connections and hydrological patterns. Treed wetlands in Type 1 land cover connections act as a thermal and hydrological buffer between peat plateaus and collapse scars, while Type 2 treed wetlands do not function as buffers. CF = channel fen; CS = collapse scar; PP = peat plateau; TW = treed wetland

these depths was saturated at the collapse scar but relatively dry at the treed wetland. As a result, the treed wetland was more thermally insulated and therefore thaw (and the return to the VWC values of the summer regime) at the 20- and 25-cm depths proceeded much more slowly than at the collapse scar (Figures 5 and S1). This effect is also evident during soil freezing, particularly at lower depths as the wettest (collapse scar) and therefore the most thermally conductive peat profile was the first to freeze and adjust to the VWC values of the winter regime.

Even though many collapse scar wetlands have developed drainage outlets due to localised permafrost thaw (Connon et al., 2015) and such outlets convey runoff during periods when the moisture supply exceeds their storage capacity, treed wetlands still drain more efficiently since runoff from them is not restricted to a single drainage outlet but can proceed in any direction leading to the collapse scar downslope. This allows treed wetlands to drain continuously rather than intermittently (i.e., when a storage threshold is exceeded). The tendency for greater efficiency of drainage from treed wetlands is supported by the greater slope of their water level recessions (Figure 8). This difference in drainage regime between treed wetlands and collapse scars facilitates the maintenance of a relatively well-developed unsaturated layer in the former and little or no unsaturated layer development in the latter. Given these contrasting hydrological characteristics, the transition from collapse scar to treed wetland therefore results in a marked change in hydrological function.

Plateau-wetland complexes (Figure 1b) dominate much of the southern margin of permafrost. Hydrologically-based classifications of this landscape type have recognised channel fens, peat plateaus and other wetlands (referred to as 'flat bogs' or 'collapse scar wetlands') as the dominant land covers (Robinson & Moore, 2000) each with characteristic hydrological functions (Hayashi et al., 2004). Subsequent studies further classified the 'other wetlands' category into wetlands that are hydrologically connected to channel fens (i.e., the basin drainage network) and those that are not (Quinton et al., 2009) and demonstrated that permafrost thaw is increasing the proportion of hydrologically-connected wetlands (Connon et al., 2014). The present study identified treed wetlands (Figure 1c), a fourth land cover type that includes areas previously misclassified as peat plateau or as collapse scar wetlands. The identification of treed wetlands, the characterisation of their physical, thermal and hydrological properties and the description of their interactions with other land cover types contribute new knowledge on how plateau-wetland complexes function hydrologically (Figure 7).

Plateau-wetland complexes contain analogues to other peatland systems. For example, the development of a treed wetland is similar to the development of a domed bog, well-documented for non-permafrost environments, whereby peat accumulation raises the ground surface (and water table) above that of the surrounding terrain to produce a peat dome that receives water through precipitation only and has a radial drainage pattern (National Wetlands Working Group [NWWG], 1997). However, despite analogues with other systems and the relatively small number of land cover types, the large spatial variations of local permafrost thaw rates and stages of land cover transition give plateau-wetland complexes a unique and spatially heterogeneous character. For example, large, compound wetlands formed from the merger of individual collapse scars of varying age are

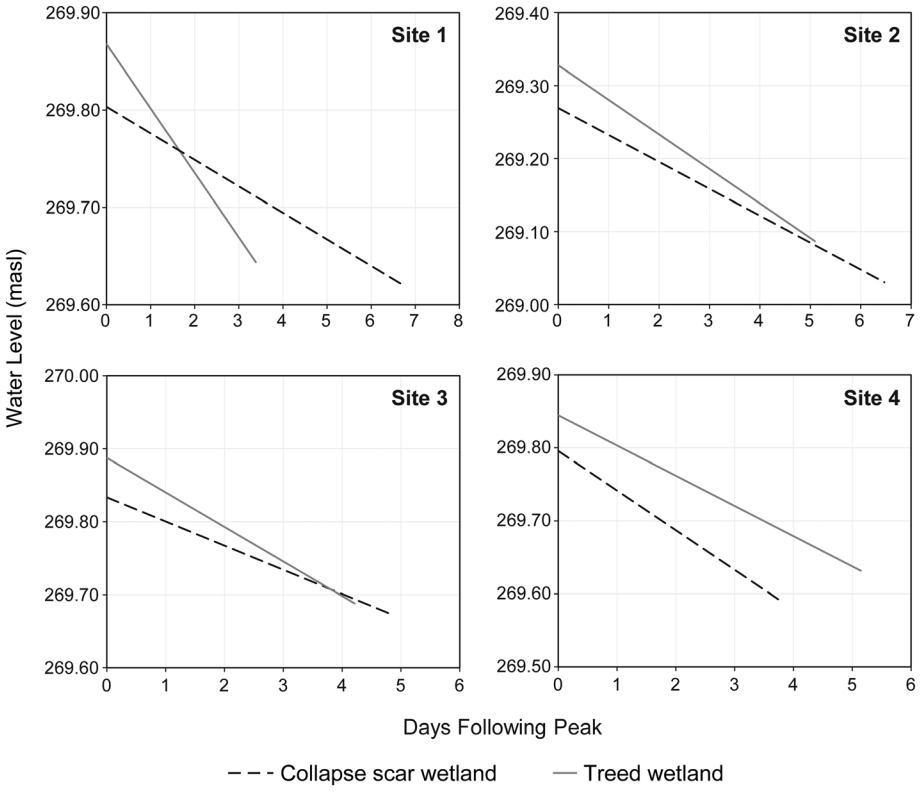

FIGURE 8 Master recession curve trend lines for each treed wetland and collapse scar wetland well. The single peat plateau well was not plotted due differences in magnitude

a common feature of these complexes. Such wetlands often contain multiple collapse scars and treed wetlands in varying stages of development, as well as areas of flooded forest and moats (i.e., along edges of thawing plateaus), and if these wetlands abut a channel fen, they may also contain fen-like (e.g., poor fen) characteristics (Figure 1b,c). Furthermore, individual features within such wetlands may themselves have complex histories. For example, examination of historical (1947 to present) aerial photography suggests that the treed wetland at Site 4 was part of a plateau that has since receded northward (Figure 1c). Inspection of this site on the ground showed that it contains both relatively young trees (of similar age to the treed wetlands of Sites 1–3) and older trees that appear to be remnants of the adjacent peat plateau or of an older collapse scar that occupied that plateau. This apparent complex history of Site 4 may in part account for why its hydrological properties and functioning differ from the other sites (e.g., Figure 8).

6 | CONCLUSION

The classical theory of the development of peat plateau forest from wetland and vice versa proposed by Zoltai (1993) and expanded upon by others is inextricably linked to local permafrost development and degradation cycles. In that context, treed wetlands represent a transitional stage leading to the development of a forested peat plateau. However, in the current context of rapid climate warming and widespread permafrost thaw, re-development of permafrost from within collapse scar wetlands is unlikely. This enables treed wetlands to persist on the landscape as a new end-member that appears to have replaced the peat plateau. Their persistence on the landscape (rather than their evolution into plateaus) has allowed the coverage of treed wetlands to increase and allowed them to attain more advanced stages of development. As demonstrated here, treed wetlands have unique hydrothermal properties that should be properly parameterized in numerical models. Considering that permafrost thaw has also been found to facilitate the de-watering of wetlands (e.g., wetland capture), ongoing drainage of treed wetlands is a positive feedback that will promote further tree growth. Since collapse scars develop from thawing permafrost, their coverage on the landscape, like that of the peat plateaus, is also expected to decrease. As such, the plateau-wetland complexes at the study site appear to be transitioning into permafrost-free black spruce forest, a common land cover type directly to the south of the study region.

ACKNOWLEDGEMENTS

We wish to thank the Dehcho First Nations, the Líídlı̨ Kų́ę́ First Nation, Jean-Marie River First Nation and Sambaa K'e First Nation for their support and acknowledge that the Scotty Creek Research Station is located on Treaty 11 land. We acknowledge funding support from ArcticNet, the Natural Sciences and Engineering Research Council of Canada (NSERC) and the Northern Scientific Training Program. We would like to thank Mason Dominico, Angela Elgie and Jessica Smart for their assistance in field data collection. We thank the two reviewers for their constructive comments.

DATA AVAILABILITY STATEMENT

The data that support the findings of this study are available from the corresponding author upon reasonable request.

ORCID

Kristine M. Haynes https://orcid.org/0000-0002-9529-4640

REFERENCES

Beilman, D. W. (2001). Plant community and diversity change due to localized permafrost dynamics in bogs of western Canada. *Canadian Journal of Botany*, *79*(8), 983–993. https://doi.org/10.1139/cjb-79-8-983

Beilman, D. W., Vitt, D. H., & Halsey, L. A. (2001). Localized permafrost peatlands in Western Canada: Definition, distributions, and degradation. *Arctic, Antarctic, and Alpine Research*, *33*(1), 70. https://doi.org/10.2307/1552279

Bourgault, M. A., Larocque, M., & Garneau, M. (2017). Quantification of peatland water storage capacity using the water table fluctuation method. *Hydrological Processes*, *31*, 1184–1195. https://doi.org/10.1002/hyp.11116

Bourgeau-Chavez, L. L., Garwood, G. C., Riordan, K., Koziol, B. W., & Slawski, J. (2010). Calibration algorithm development for selected water content reflectometers to burned and non-burned organic soils of Alaska. *International Journal of Wildland Fire*, *19*, 961–975. https://doi.org/10.1071/WF07175

Camill, P. (1999). Peat accumulation and succession following permafrost thaw in the boreal peatlands of Manitoba, Canada. *Écoscience*, *6*(4), 592–602. https://doi.org/10.1080/11956860.1999.11682561

Camill, P. (2005). Permafrost thaw accelerates in boreal peatlands during late-20th century climate warming. *Climatic Change*, *68*(1–2), 135–152. https://doi.org/10.1007/s10584-005-4785-y

Camill, P., Lynch, J. A., Clark, J. S., Adams, J. B., & Jordan, B. (2001). Changes in biomass, aboveground net primary production, and peat accumulation following permafrost thaw in the boreal peatlands of Manitoba. *Canada. Ecosystems*, *4*, 461–478. https://doi.org/10.1007/s10021-001-0022-3

Carpino, O. A., Berg, A. A., Quinton, W. L., & Adams, J. R. (2018). Climate change and permafrost thaw-induced boreal forest loss in northwestern Canada. *Environmental Research Letters*, *13*, 084018. https://doi.org/10.1088/1748-9326/aad74e

Chasmer, L., & Hopkinson, C. (2017). Threshold loss of discontinuous permafrost and landscape evolution. *Global Change Biology*, *23*, 2672–2686. https://doi.org/10.1111/gcb.13537

Chasmer, L., Hopkinson, C., & Quinton, W. (2010). Quantifying errors in historical permafrost plateau change in the Canadian sub-arctic from aerial photography and airborne lidar: 1947 to present. *Canadian Journal of Remote Sensing*, *36*(2), S211–S223. https://doi.org/10.5589/m10-058

Connon, R., Devoie, É., Hayashi, M., Veness, T., & Quinton, W. (2018). The influence of shallow taliks on permafrost thaw and active layer dynamics in subarctic Canada. *Journal of Geophysical Research: Earth Surface*, *123*(2), 281–297. https://doi.org/10.1002/2017JF004469

Connon, R. F., Quinton, W. L., Craig, J. R., Hanisch, J., & Sonnentag, O. (2015). The hydrology of interconnected bog complexes in discontinuous permafrost terrains. *Hydrological Processes*, *29*(18), 3831–3847. https://doi.org/10.1002/hyp.10604

Connon, R. F., Quinton, W. L., Craig, J. R., & Hayashi, M. (2014). Changing hydrologic connectivity due to permafrost thaw in the lower Liard River valley, NWT, Canada. *Hydrological Processes*, *28*, 4163–4178. https://doi.org/10.1002/hyp.10206

Devoie, É. G., Craig, J. R., Connon, R. F., & Quinton, W. L. (2019). Taliks: A tipping point in discontinuous permafrost degradation in peatlands. *Water Resources Research*, *55*(11), 9838–9857. https://doi.org/10.1029/2018WR024488

FitzGibbon, J. E. (1981). Thawing of seasonally frozen ground in organic terrain in Central Saskatchewan. *Canadian Journal of Earth Sciences*, *18*, 1492–1496. https://doi.org/10.1139/e81-139

Garon-Labrecque, M.-È., Léveillé-Bourret, É., Higgins, K., & Sonnentag, O. (2015). Additions to the boreal flora of the Northwest Territories with a preliminary vascular flora of Scotty Creek. *Canadian Field-Naturalist*, *129*(4), 349–367.

Gordon, J., Quinton, W., Branfireun, B. A., & Olefeldt, D. (2016). Mercury and methylmercury biogeochemistry in a thawing permafrost wetland complex, Northwest Territories, Canada. *Hydrological Processes*, *30*, 3627–3638. https://doi.org/10.1002/hyp.10911

Government of the Northwest Territories [GNWT]. (2018). 2030 NWT Climate Change Strategic Framework. https://www.enr.gov.nt.ca/sites/enr/files/resources/128-climate_change_strategic_framework_web.pdf

Halsey, L. A., Vitt, D. H., & Zoltai, S. C. (1995). Disequilibrium response of permafrost in boreal continental western Canada to climate change. *Climatic Change*, *30*(1), 57–73. https://doi.org/10.1007/BF01093225

Hayashi, M., Goeller, N., Quinton, W. L., & Wright, N. (2007). A simple heat-conduction method for simulating the frost table depth in hydrological models. *Hydrological Processes*, *21*, 2610–2622. https://doi.org/10.1002/hyp.6792

Hayashi, M., Quinton, W. L., Pietroniro, A., & Gibson, J. J. (2004). Hydrologic functions of wetlands in a discontinuous permafrost basin indicated by isotopic and chemical signatures. *Journal of Hydrology*, *296*(1–4), 81–97. https://doi.org/10.1016/j.jhydrol.2004.03.020

Haynes, K. M., Connon, R. F., & Quinton, W. L. (2018). Permafrost thaw induced drying of wetlands at Scotty Creek, NWT, Canada. *Environmental Research Letters*, *13*(11), 114001. https://doi.org/10.1088/1748-9326/aae46c

Haynes, K. M., Connon, R. F., & Quinton, W. L. (2019). Hydrometeorological measurements in peatland-dominated, discontinuous permafrost at Scotty Creek, Northwest Territories, Canada. *Geoscience Data Journal*, *6*(2), 85–96. https://doi.org/10.1002/gdj3.69

Haynes, K. M., Smart, J., Disher, B., Carpino, O., & Quinton, W. L. (2020). The role of hummocks in re-establishing black spruce forest following permafrost thaw. *Ecohydrology*, *14*(3), e2273. https://doi.org/10.1002/eco.2273

Helbig, M., Wischnewski, K., Kljun, N., Chasmer, L. E., Quinton, W. L., Detto, M., & Sonnentag, O. (2016). Regional atmospheric cooling and wetting effect of permafrost thaw-induced boreal forest loss. *Global Change Biology*, *2*(12), 4048–4066. https://doi.org/10.1111/gcb.13348

Jorgenson, M. T., Romanovsky, V., Harden, J., Shur, Y., O'Donnell, J., Schuur, E. A. G., Kanevskiy, M., & Marchenko, S. (2010). Resilience and vulnerability of permafrost to climate change. *Canadian Journal of Forest Research*, *40*(7), 1219–1236. https://doi.org/10.1139/X10-060

Kneisel, C., Hauck, C., Fortier, R., & Moorman, B. (2008). Advances in geophysical methods for permafrost investigations. *Permafrost and Periglacial Processes*, *19*(2), 157–178. https://doi.org/10.1002/ppp.616

Kwong, J., & Gan, T. (1994). Northward migration of permafrost along the Mackenzie highway and climate warming. *Climatic Change*, *26*, 399–419. https://doi.org/10.1007/BF01094404

Lewkowicz, A. G., Etzelmüller, B., & Smith, S. L. (2011). Characteristics of discontinuous permafrost based on ground temperature measurements and electrical resistivity tomography, southern Yukon, Canada. *Permafrost and Periglacial Processes*, *22*(4), 320–342. https://doi.org/10.1002/ppp.703

Lieffers, V. J., & Rothwell, R. L. (1987). Rooting of peatland black spruce and tamarack in relation to depth of water table. *Canadian Journal of Botany*, *65*, 817–821. https://doi.org/10.1139/b87-111

Marks, D., Kimball, J., Tingey, D., & Link, T. (1998). The sensitivity of snowmelt processes to climate conditions and forest cover during rain-on-snow: A case study of the 1996 Pacific northwest flood. *Hydrological Processes*, *12*, 1569–1587. https://doi.org/10.1002/(SICI)1099-085(199808/09)12:10/11%3C1569::AID-HYP682%3E3.0.CO;2-L

McClymont, A. F., Hayashi, M., Bentley, L. R., & Christensen, B. S. (2013). Geophysical imaging and thermal modeling of subsurface morphology and thaw evolution of discontinuous permafrost. *Journal of Geophysical Research: Earth Surface*, *118*(3), 1826–1837. https://doi.org/10.1002/jgrf.20114

Menberu, M. W., Tahvanainen, T., Marttila, H., Irannezhad, M., Ronkanen, A. -K., Penttinen, J., & Klove, B. (2016). Water-table-dependent hydrological changes following peatland forestry drainage and restoration: Analysis of restoration success. *Water Resources Research*, *52*, 3742–3760. https://doi.org/10.1002/2015WR018578

Meteorological Service of Canada (MSC). (2017). *National climate data archive of Canada*. Dorval, Quebec, Canada: Environment Canada.

National Wetlands Working Group (NWWG). (1997). In B. G. Warner & C. D. A. Rubec (Eds.), *The Canadian wetland classification system* (p. 68). Waterloo, Ontario: University of Waterloo Press.

Nungesser, M. K. (2003). Modelling microtopography in boreal peatlands: Hummocks and hollows. *Ecological Modelling*, *165*(2–3), 175–207. https://doi.org/10.1016/S0304-3800(03)00067-X

Parazoo, N. C., Koven, C. D., Lawrence, D. M., Romanovsky, V., & Miller, C. E. (2018). Detecting the permafrost carbon feedback: Talik formation and increased cold-season respiration as precursors to sink-to-source transitions. *The Cryophere*, *12*, 123–144. https://doi.org/10.5194/tc-12-123-2018

Payette, S., Delwaide, A., Caccianiga, M., & Beauchemin, M. (2004). Accelerated thawing of subarctic peatland permafrost over the last 50 years. *Geophysical Research Letters*, *31*(18), 1–4. https://doi.org/10.1029/2004GL020358

Posavec, K., Bačani, A., & Nakić, Z. (2006). A visual basic spreadsheet macro for recession curve analysis. *Groundwater*, *44*(5), 764–767. https://doi.org/10.1111/j.1745-6584.2006.00226.x

Quinton, W., Berg, A., Braverman, M., Carpino, O., Chasmer, L., Connon, R., Craig, J., Devoie, É., Hayashi, M., Haynes, K., Olefeldt, D., Pietroniro, A., Rezanezhad, F., Schincariol, R., & Sonnentag, O. (2019). A synthesis of three decades of hydrological research at Scotty Creek, NWT, Canada. *Hydrology and Earth System Sciences*, *23*, 2015–2039. https://doi.org/10.5194/hess-23-1-2019

Quinton, W. L., Hayashi, M., & Chasmer, L. E. (2009). Peatland hydrology of discontinuous permafrost in the Northwest Territories: Overview and synthesis. *Canadian Water Resources Journal*, *34*, 311–328. https://doi.org/10.4296/cwrj3404311

Quinton, W. L., Hayashi, M., & Chasmer, L. E. (2011). Permafrost-thaw-induced land-cover change in the Canadian subarctic: Implications for water resources. *Hydrological Processes*, *25*(1), 152–158. https://doi.org/10.1002/hyp.7894

Quinton, W. L., Hayashi, M., & Pietroniro, A. (2003). Connectivity and storage functions of channel fens and flat bogs in northern basins. *Hydrological Processes*, *17*(18), 3665–3684. https://doi.org/10.1002/hyp.1369

Quinton, W. L., Shirazi, T., Carey, S. K., & Pomeroy, J. W. (2005). Soil water storage and active-layer development in a sub-alpine tundra hillslope, southern Yukon territory, Canada. *Permafrost and Periglacial Processes*, *16*, 369–382. https://doi.org/10.1002/ppp.543

R Core Development Team, Version 3.5.2. (2018). *R: A language and environment for statistical computing*. Vienna, Austria. URL: R foundation for statistical computing. http://www.R-project.org/

Robinson, S. D., & Moore, T. R. (2000). The influence of permafrost and fire upon carbon accumulation in high boreal peatlands, Northwest Territories, Canada. *Arctic, Antarctic, and Alpine Research*, *32*(2), 155–166. https://doi.org/10.2307/1552447

Shur, Y. L., & Jorgenson, M. T. (2007). Patterns of permafrost formation and degradation in relation to climate and ecosystems. *Permafrost and Periglacial Processes*, *18*(1), 7–19. https://doi.org/10.1002/ppp.582

Tallaksen, L. M. (1995). A review of baseflow recession analysis. *Journal of Hydrology*, *165*(1–4), 349–370. https://doi.org/10.1016/0022-1694(94)02540-R

Tarnocai, C. (2009). The impact of climate change on Canadian peatlands. *Canadian Water Resources Journal*, *34*, 453–466. https://doi.org/10.4296/cwrj3404453

Vitt, D. H., Halsey, L. A., & Zoltai, S. C. (1994). The bog landforms of continental western Canada in relation to climate and permafrost patterns. *Arctic and Alpine Research*, *26*(1), 1–13. https://doi.org/10.2307/1551870

Vonk, J. E., Tank, S. E., & Walvoord, M. A. (2019). Integrating hydrology and biogeochemistry across frozen landscapes. *Nature Communications*, *10*, 5377. https://doi.org/10.1038/s41467-019-13361-5

Waddington, J. M., Morris, P. J., Kettridge, N., Granath, G., Thompson, D. K., & Moore, P. A. (2015). Hydrological feedbacks in northern peatlands. *Ecohydrology*, *8*(1), 113–127. https://doi.org/10.1002/eco.1493

Walvoord, M. A., Voss, C. I., Ebel, B. A., & Minsley, B. J. (2019). Development of perennial thaw zones in boreal hillslopes enhances potential mobilization of permafrost carbon. *Environmental Research Letters*, *14*, 015003. https://doi.org/10.1088/1748-9326/aaf0cc

Zoltai, S. C. (1993). Cyclic development of permafrost in the peatlands of northwestern Canada. *Arctic and Alpine Research*, *25*(3), 240–246. https://doi.org/10.2307/1551820

SUPPORTING INFORMATION

Additional supporting information may be found online in the Supporting Information section at the end of this article.

How to cite this article: Disher BS, Connon RF, Haynes KM, Hopkinson C, Quinton WL. The hydrology of treed wetlands in thawing discontinuous permafrost regions. *Ecohydrology*. 2021;e2296. https://doi.org/10.1002/eco.2296